UNCONVENTIONAL EDGE DETECTOR: PRELIMINARY THEORETICAL INVESTIGATION

R Chandrasekhar, P Houlis and Y Attikiouzel

Australian Research Centre for Medical Engineering
The University of Western Australia
35 Stirling Highway, Crawley, WA 6009, Australia
chandra|pantazis|yianni@ee.uwa.edu.au

Abstract: We have recently described a range-based neighbourhood operator and an experimentally discovered unconventional edge detector based on it. The latter relies on data fitting in a pixel neighbourhood, and has a wide dynamic range. A preliminary theoretical investigation of its basis, and some of its properties, are presented in this paper. It is revealed that the edge sensitive feature is the range of pixel values in successive pixel annuli around a central pixel. It is also shown that the edge strength at any centre pixel may be approximated, in the first instance, by the sum of the logarithms of these annular range values. The derived approximation is illustrated with a synthetic image and a mammogram.

1. INTRODUCTION

We have recently described a range-based neighbourhood operator [1] and an unconventional edge detector [2] based on it. These papers extended the work first described by Russ in 1990 [3] to characterize local texture.

The unconventional edge detector is based on the data analysis and curve fitting of pixels, from a neighbourhood of a central pixel, and has some interesting properties, including a wide dynamic range and possible insensitivity to noise. A preliminary investigation into the basis of the edge detector is presented in this paper, and illustrated with examples. We begin some notation and a brief definition of the edge detector.

2. NOTATION

A digital image $I : \mathbb{Z} \times \mathbb{Z} \rightarrow \mathbb{Z}$ is defined on a compact lattice in $\mathbb{Z}^2$ with integer-valued *pixels* in some pre-defined finite co-domain in $\mathbb{Z}$. We next define a *neighbourhood* $N = N_r^t(\mathbf{p})$ as a region of symmetrically distributed pixels $\mathbf{q}$, around a pre-defined *centre pixel* $\mathbf{p} \in I$, up to a *radius* r from $\mathbf{p}$, defined using the Minkowski t-norm, $\|\cdot\|_t$ on $\mathbb{R}^2$ so $\|\mathbf{p}-\mathbf{q}\|_t = \left[\sum_{i=1}^{2} |\mathbf{p}-\mathbf{q}|^t\right]^{\frac{1}{t}} \leq r$. The two-dimensional neighbourhoods corresponding to Minkowski t-norms on $\mathbb{R}^2$ with $t = 1, 2$ and ∞ have the shape of a diamond, circle, and square, respectively [4].

Each pixel that belongs to a neighbourhood is labelled by a value d_i which denotes its *distance,* or norm value, from the centre pixel, for the chosen norm, t. Note that there are $n = |\{d_i\}|$ *distinct distances* which can be ordered so: $1 = d_1 < d_2 <, \ldots, < d_n = r$. For each d_i there exists a set $S_i(\mathbf{p})$ of *all* pixels which lie at that fixed distance from the centre pixel $\mathbf{p}$, i.e., $S_i(\mathbf{p}) = \{\mathbf{q} : \|\mathbf{p}-\mathbf{q}\|_t = d_i\}$.

Let ${s_i}^{\max}$ and ${s_i}^{\min}$ be the corresponding maximum and minimum *values* of the pixels in $S_i(\mathbf{p})$.

We then define the *range* $R_i(\mathbf{p})$ for the pixels at a distance d_i from the centre pixel $\mathbf{p}$ to be $R_i(\mathbf{p}) = {s_i}^{\max} - {s_i}^{\min}$. Finally, we define the cardinality of the neighbourhood $|N|$ to be the *total* number of pixels inside the neighbourhood N, which also represents the number of pixels that contribute to the mathematical operation around the centre pixel. The above procedure is repeated for all $\mathbf{p}$ in I.

3. UNCONVENTIONAL EDGE DETECTOR

Using the above notation, for any central pixel $\mathbf{p}$, we get a total of n range values, $R_1, \ldots, R_n$ corresponding to n unique distances $d_1, \ldots, d_n$. A straight line is fitted to a plot of the n data-pairs $\log_{10} R_i$ versus $\log_{10} d_i$ so as to minimize the square of the error. For convenience, we shall abbreviate $\log_{10}$ to log. Note that the d_is are not random variables, but the R_is are. The interested reader is referred to Draper and Smith [5] for further details on regression analysis.

The gradient m, y-axis intercept c, and the square of coefficient of correlation η^2 of the fitted straight line are given by [5]:

$$m = \frac{n\sum(\log d_i \log R_i) - (\sum \log d_i)(\sum \log R_i)}{n\sum(\log d_i)^2 - (\sum \log d_i)^2} \quad (1)$$

$$c = \frac{\sum \log R_i}{n} - m\frac{\sum \log d_i}{n} \quad (2)$$

$$\eta^2 = \left(\frac{\sum[(\log d_i - \bar{d})(\log R_i - \bar{R})]}{\sqrt{\sum(\log d_i - \bar{d})^2}\sqrt{\sum(\log R_i - \bar{R})^2}} \right)^2 \quad (3)$$

where $\bar{d} = \frac{\sum \log d_i}{n}$, $\bar{R} = \frac{\sum \log R_i}{n}$ are the mean values for $\log d_i$ and $\log R_i$ correspondingly, and the summations are understood to be $\sum_{i=1}^{n}$.

We now define the *range-based neighbourhood operator* [1] as follows. For every pixel $\mathbf{p}$ in an image $I : \mathbb{Z} \times \mathbb{Z} \rightarrow \mathbb{Z}$ with a given neighbourhood $N = N_r^t(\mathbf{p})$ of radius r, centre pixel $\mathbf{p}$ and norm t, we define the edge

0-7803-7503-3/02/$17.00 ©2002 IEEE

operator $\mathcal{N}$ to be

$$\mathcal{N}(t,r,\mathbf{p}) = \begin{pmatrix} m \\ c \\ \eta^2 \end{pmatrix} \tag{4}$$

where m, c and η^2 are correspondingly the gradient, the y-axis intercept and the square of the coefficient of correlation as defined above. The edge sensitive component of the RHS of equation (4) is the y-axis intercept, c. For a geometrical definition of this operator the interested reader is referred to a previous publication of ours [1].

The *unconventional edge detector* $\mathcal{E}$ maps the centre pixel $\mathbf{p}$ to the y-axis intercept alone and is therefore defined as:

$$\mathcal{E}(t,r,\mathbf{p}) = c = \frac{\sum \log R_i}{n} - m\frac{\sum \log d_i}{n} \tag{5}$$

For succinctness, when the edge operator is applied to an entire image, I, we shall denote the resulting image by $\mathcal{E}(t,r,I)$.

4. MATHEMATICAL ANALYSIS

Hereafter, t is assumed to be 2. The following notational simplification is introduced to facilitate analysis of equation (5):

$$dS_1 = \sum \log d_i, \quad dS_2 = \sum (\log d_i)^2, \quad D = n dS_2 - dS_1{}^2$$

For a given neighbourhood $N_r^t(\mathbf{p})$, each of dS_1, dS_2, and D is known. For example, if we set $r = 3$, we have:

i	d_i	n	dS_1	dS_2	D
1	1.0000				
2	1.4142				
3	2.0000				
4	2.2361	6	3.9828	3.5361	5.3542
5	2.8284				
6	3.0000				

Substituting for m into equation (2) for c, we get

$$\begin{aligned}
m &= \frac{1}{D}\left[n\sum(\log d_i \log R_i) - \left(\sum \log d_i\right)\left(\sum \log R_i\right)\right] \\
c &= \frac{1}{n}\left[\sum \log R_i - m\sum \log d_i\right] \\
&= \frac{1}{nD}\left[\left(\sum \log R_i\right) n\sum (\log d_i)^2 - \left(\sum \log R_i\right)\left(\sum \log d_i\right)^2\right. \\
&\left. - n\sum(\log d_i \log R_i)\left(\sum \log d_1\right) + \left(\sum \log d_i\right)^2\left(\sum \log R_i\right)\right] \\
&= \frac{1}{D}\left[\sum(\log R_i)\sum(\log d_i)^2 - \sum(\log R_i \log d_i)\left(\sum \log d_i\right)\right] \\
&= \frac{1}{D}\left[dS_2\sum(\log R_i) - dS_1\sum(\log R_i \log d_i)\right] \\
&= \frac{1}{D}\sum \log R_i^{(dS_2 - dS_1 \log d_i)}
\end{aligned} \tag{6}$$

The exponent $(dS_2 - dS_1 \log d_i)$ in equation (6) is independent of the pixel values in N, or equivalently, is *independent of position*, because dS_1 and dS_2 are known positive constants that vary not with position $\mathbf{p}$ but with radius r.

To better understand the behaviour of the exponent $(dS_2 - dS_1 \log d_i)$, it is plotted against d_i, as illustrated in Figure 1. We conclude that as i increases, i.e., as we

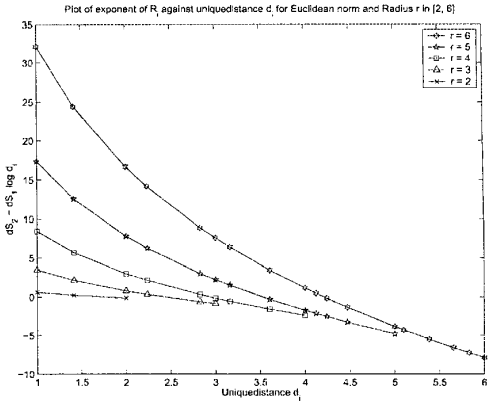

Fig. 1. The term $(dS_2 - dS_1 \log d_i)$ is plotted against d_i for radii $r = 2,3,4,5,6$. As $i \to n$, $(dS_2 - dS_1 \log d_i)$ decreases, i.e., distant pixels contribute less to the edge strength. However, as r increases, the contribution of pixels near the centre pixel is amplified.

get further away from the centre pixel, the contribution of the range R_i to the value c is correspondingly diminished. The exponent $(dS_2 - dS_1 \log d_i)$ therefore *modulates* the values $\log R_i$ with distance d_i from the centre pixel. Moreover, as radius r increases, the contribution of pixels close to the centre pixel is amplified.

An analytical expression for the exponent will depend on the radius r and the chosen norm t. The number n of unique distances plays a pivotal role in this analysis. The value n as a function of r is still under investigation. However, there is an upper bound of $\frac{(r+1)(r+2)}{2}$ and a lower bound of $\frac{(r+1)(r+2)}{4}$ on n as illustrated in Figure 2.

Meanwhile, as a first approximation, we propose setting the exponent to a constant, say, 1. We then get the *approximate* equation for c, namely

$$c \approx \frac{1}{D}\sum \log R_i. \tag{7}$$

It may then be hypothesized that the unconventional edge detector works by accumulating the logarithms of the ranges in successive annuli around the centre pixel.

5. EXPERIMENTAL RESULTS

Experiments were performed with synthetic and real images using the unconventional edge detector in its exact form (6) and also the approximation derived in equation (7). These are described below.

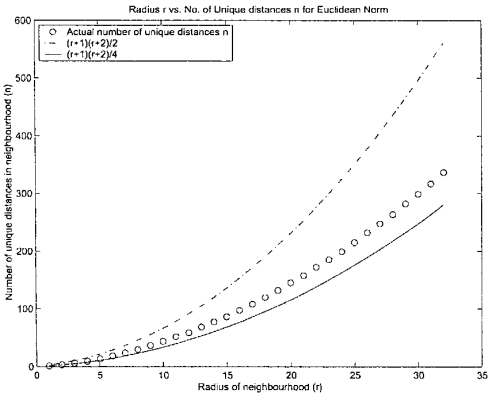

Fig. 2. Variation of unique distances n with radius of neighbourhood r for the Euclidean or 2-norm. Note that for r in [1, 32], n has an upper bound of $(r+1)(r+2)/2$ and a lower bound of $(r+1)(r+2)/4$.

Fig. 3. Results with synthetic images. The original image is an intensity step edge. The exact edge is that detected by the unconventional edge detector for $r = 4$. Note that it is symmetrical about the original edge. The approximate edge detected using the approximation in equation (7) appears "smeared out".

5.1. Synthetic edge: intensity interface

A binary synthetic image was considered, in which the edge is the interface between two iso-intensity regions having different pixel values, set to a and b with $a > b$ without loss of generality. The only possible values for the R_is are either $(a-b)$ or 0. The distribution of range values will depend on the position of the centre pixel, i.e., whether it lies in an entirely homogeneous region, or across a transition, and on the radius r. The original synthetic image and the results from the exact and approximate edge detectors are shown in Figure 3.

5.2. Medical image: mammogram

When an original mammogram M is subjected to the unconventional edge detector, the resulting image $\mathcal{E}(4,2,M)$ is shown in the centre of Figure 4 while the approximation in equation (7) results in the right image in that figure.

6. DISCUSSION

With a binary synthetic step image, we should expect to see a two-pixel wide response for any step transition

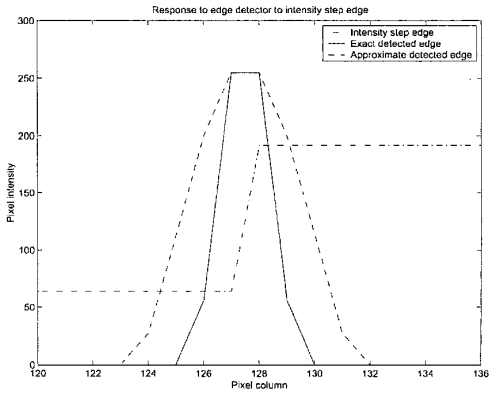

Fig. 5. Edge profiles for synthetic intensity step edge image. These graphs correspond to interpolated pixel profiles across the three images in Figure 3.

purely because of symmetry considerations. From equation (7), as the centre pixel recedes away from the edge, or intensity transition, the number of non-zero ranges R_i decreases, and so will the intensity of the centre pixel in the edge image. Ultimately, when the neighbourhood around the centre pixel lies entirely in an iso-intensity region, there will be no non-zero ranges, and the edge strength will be zero. So we would expect to see a symmetrical edge that tapers off in intensity gradually with increasing distance from the step edge, finally becoming zero. This effect is seen in Figure 5. Moreover, the number of "auxiliary edges" around the actual central edge increases with radius r, so that edge images resulting from large r have thick, blurred-looking edges.

Like the synthetic edge images, the mammogram edge images are crisper for the exact, and more blurred for the approximate versions respectively.

For a more quantitative understanding of the images in Figure 3, we note that $n \propto r^2$, i.e., the number of unique distances n grows at a rate of r^2 as has been demonstrated in Figure 2. Thus the transition is steep for $r = 4$, but less steep for the approximation, for reasons which are still being investigated. The values of the exponent $(dS_2 - dS_1 \log d_i)$ for $i \to r$ are negative, showing negligible influence from the ranges R_i of pixels which lie far from the centre of the neighbourhood.

From equation (7), we may assert that the unconventional edge detector relies upon the range of pixel values in a discrete annulus around a centre pixel as its edge-sensitive *feature*. The logarithm *function* scales the range response so that *low* intensity edges that are usually not visible are made visually perceptible a logarithmically compressed edge image of wider dynamic range than is possible with a linear edge image.

The approximation derived in this paper has been presented, not only mathematically, but also visually, for comparison with the exact edge image from $\mathcal{E}$. The approximated image appears blurred and displays a thicker edge, but is otherwise similar to the exact image, thereby

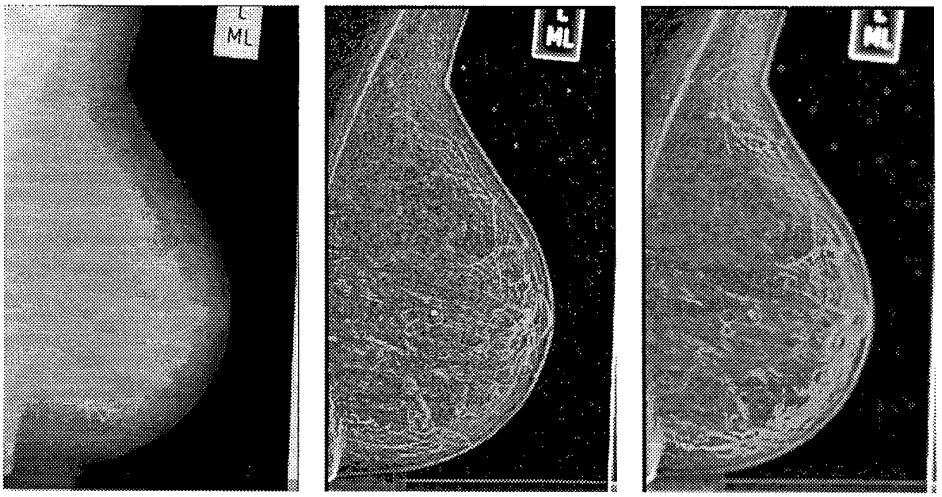

Original Exact edge Approximate edge

Fig. 4. Results with mammograms. Note how edges invisible on the original on the left are rendered visible on the edge images, illustrating the wide dynamic range of the edge detector. The exact edge image appears crisper then the approximate edge image.

validating the approximation.

The effects of the *annular* accumulation of range values, of *scale,* and of *noise* need to be further investigated. It would also be interesting to assess the effect of the norm on the results, and to select the optimal one, if it exists. Finally, consideration should be given to varying both the feature and function beyond the current choices of range and logarithm.

7. CONCLUSIONS

We have presented a preliminary theoretical investigation of the unconventional edge detector. The y-axis intercept of a log-log fit of annular range against Euclidean distance from the centre pixel in a neighbourhood has been shown, in the first instance, to be approximately proportional to the sum of the logarithm of pixel range values in discrete annuli. This approximation has been derived mathematically, and its validity, demonstrated visually.

Acknowledgements

This research was partially supported by Australian Research Council (ARC) Large Grant No. A00000714 and by the Western Australian Government through funding of ARCME as part of its *Centres of Excellence* programme.

REFERENCES

[1] R. Chandrasekhar and Y. Attikiouzel, "New range-based neighbourhood operator for extracting edge and texture information from mammograms for subsequent image segmentation and analysis," *IEE Proceedings—Science, Measurement and Technology*, vol. 147, pp. 408–413, Nov. 2000.

[2] R. Chandrasekhar and Y. Attikiouzel, "Unconventional edge detector," *Electronics Letters*, vol. 37, pp. 79–80, Jan. 2001.

[3] J. C. Russ, "Processing Images with a Local Hurst Operator to Reveal Textural Differences," *Journal of Computer Assisted Microscopy*, vol. 2, no. 4, pp. 249–257, 1990.

[4] R. O. Duda and P. E. Hart, *Pattern Classification and Scene Analysis*. New York: John Wiley and Sons, 1973.

[5] N. R. Draper and H. Smith, *Applied Regression Analysis*. New York, USA: John Wiley and Sons, 3rd ed., 1998.